

12th CIRP Conference on Intelligent Computation in Manufacturing Engineering, 18-20 July 2018,  
Gulf of Naples, Italy

# Workpiece positioning sensor (wPOS): A three-degree-of-freedom relative end-effector positioning sensor for robotic manufacturing

Thomas O.H. Charrett<sup>a,\*</sup>, Thomas Kissinger<sup>a</sup>, Ralph P. Tatam<sup>a</sup>

<sup>a</sup>Centre for Engineering Photonics, Cranfield University, MK43 0AL, UK

\* Corresponding author. Tel.: +44 1234 758205; E-mail address: [t.charrett@cranfield.ac.uk](mailto:t.charrett@cranfield.ac.uk)

## Abstract

This paper reports on the development of a new, non-contact, cost-effective and widely-applicable optical sensor for the measurement of the three degrees of translational freedom of a robotic end-effector. The workpiece positioning sensor (wPOS) tracks the relative position between the workpiece and end-effector in real-time, using laser speckle correlation for the measurement of in-plane position and Range-Resolved Interferometry for out-of-plane positioning. The sensing principles of the techniques and the development of the instrument are discussed along with example results for applications in robotic additive manufacturing for tool speed and layer height measurements.

© 2019 The Authors. Published by Elsevier B.V.

This is an open access article under the CC BY license (<https://creativecommons.org/licenses/by/3.0/>)

Peer-review under responsibility of the scientific committee of the 12th CIRP Conference on Intelligent Computation in Manufacturing Engineering.

**Keywords:** Displacement sensing; Process monitoring; Positioning; Tool path; Tool speed; Laser speckle; Interferometry; Range Resolved Interferometry

## 1. Introduction

In many areas of manufacturing it is desirable to replace expensive Computer Numerical Control (CNC) Cartesian systems with a robotic approach providing increased flexibility and lower costs. However, robots struggle to achieve high positioning accuracy and are more prone to disturbances from process forces due to the comparatively low mechanical stiffness of typical industrial robots [1]. Additionally, there can be significant deviations from the desired tool-path and tool-speed that are not captured by the kinematic models used to convert joint encoder positions to Cartesian end-effector position.

Hence, characterization of the robot motion is of great importance in many manufacturing operations, for example, in many continuous machining or processing operations the feed rate or tool speed is critical to ensure process quality [2] while in contact tasks, such as polishing and drilling, the comparatively low mechanical stiffness of typical industrial robots can result in excessive tool slippage and vibration resulting in errors in dimension and/or poor surface quality, with deflections of up to 0.25mm reported in robotic milling

operations [3]. Finally, in other areas there is a demand for higher precision in-process feedback. For example, in additive manufacturing there is a need for on-line process monitoring such as deposition layer height measurements and control of disturbances during deposition [4], while in laser cutting, control of the focus position relative to the workpiece is critical to ensure cut quality [5].

To help open up these applications to robots improved sensors and instrumentation are required to provide feedback on the position of robotic end-effectors relative to the workpiece. External measurements systems such as laser trackers, iGPS or vision system can be used to track the motion of the robot end-effector. However, these methods of monitoring robot motion also suffer from limitations; vision systems have limited update rates, while laser scanners are expensive and inflexible due to the need to maintain a continuous line-of-sight.

In this paper we report on the development of a new non-contact and widely applicable, optical instrument for the non-contact measurement of the relative position between a robot and the workpiece. This instrument, the workpiece Positioning sensor (wPOS) aims to be a relatively low-cost

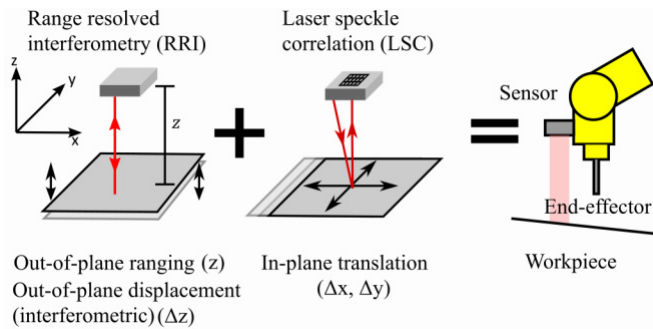


Fig. 1. Operating concept of the wPOS instrument combining Range Resolved Interferometry (RRI) and Laser Speckle Correlation sensing (LSC).

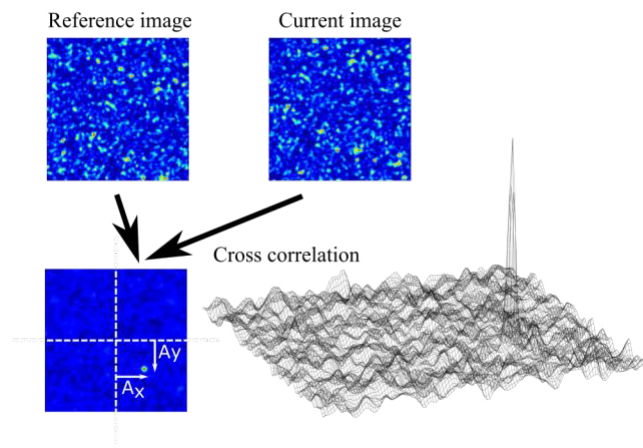


Fig. 2. Operating principle of Laser speckle correlation.

alternative to laser scanners, providing a range of positional feedback information for robotic processes.

In the following sections the operating principle of the wPOS instrument is described, and typical performance characteristics in various application areas and modes of operation are discussed, with example results from early application trials also presented.

## 2. Theory of Operation

The general concept behind of the instrument consists of an end-effector mounted sensor head that allows the measurement in real-time of the relative position between the robotic end-effector and the workpiece in three translational degrees-of-freedom ( $x, y, z$ ). To achieve this aim, two complimentary optical non-contact measurement techniques are combined with the principle also shown in Fig. 1. Range resolved interferometry (RRI) [6], Fig. 1 (a), allows the measurement of the out-of-plane motion while Laser Speckle Correlation (LSC) [7,8], Figure 1 (b) is used for the measurement of the in-plane motion ( $x, y$ ) and potentially in-plane rotation [9].

### 2.1. Range resolved interferometry (RRI)

Range-resolved interferometry (RRI) [6] is a cost-effective interferometry technique based on the sinusoidal wavelength

modulation of widely available and robust telecoms laser diodes. This allows high-quality measurement of the interferometric phase giving typically nm level resolution in displacement measurements at multi-kHz bandwidths. In common with other interferometric methods this allows only relative displacement measurements referenced to a starting position and not the absolute range. However the range-resolving properties of the technique enables discrimination between signals originating at different ranges and this allows the additional lower-resolution measurement of the absolute distance at typically 10 to 100  $\mu\text{m}$  resolution

To obtain absolute distance measurements the return signal strength is evaluated as a function of range using a Gaussian peak fit, while the displacement measurements are obtained by selecting a peak and applying quadrature demodulation to obtain interferometric phase information [6].

In the wPOS instrument, the RRI measurement beam is arranged to measure the workpiece-end-effector distance - with both interferometric displacement and absolute range measurement modes simultaneously available. Here the optical interferometer is made between the fibre tip and the workpiece surface, making the interferometer insensitive to common path changes in the delivery/collection optical fibre.

Compared to competing distance sensors, such as laser triangulation and chromatic confocal approaches [10], RRI-based sensors offer large dynamic working ranges ( $\geq 10\text{cm}$ ) at flexible stand-off distances and permit the realization of very compact sensor heads ( $\leq 10\text{mm}$  diameter), consisting solely of a simple beam-conditioning lens. Another key feature of the technique is that as an interferometric technique it is immune to background process light and has been successfully applied in the presence of arc-weld light – see example application in section 3.2 below.

### 2.2. Laser speckle correlation (LSC)

The in-plane positioning is achieved by the use of high-speed laser speckle correlation (LSC) [7,8]. The concept of this approach is shown in Fig. 1 a) where the sensor consisting of a laser source and array detector/camera is attached to the robot end-effector.

The workpiece surface is illuminated with a laser and the resulting scattered light pattern recorded by a camera. No imaging lens is necessary; rather the camera is used as an array detector to sample the resulting scattered light field – the objective laser speckle pattern. An example of such a recorded speckle pattern is shown in Fig. 2 which also illustrates the signal processing principle used. This consists of tracking the translation of the acquired speckle pattern at high speed ( $\sim 500\text{fps}$ ) via the application of the two-dimensional normalized cross-correlation [11]. The offset of the peak from the center of the correlation image yields the shift of the speckle pattern, ( $A_x, A_y$ ) which can then be related to the  $x$  and  $y$  translations between the sensor and workpiece occurring between the images. It should be noted that the laser speckle patterns used by the sensor can be formed from a wide variety of surfaces as long as the surface is rough at the scale of the optical wavelength ( $\sim 0.7\mu\text{m}$ ), i.e. any diffusely

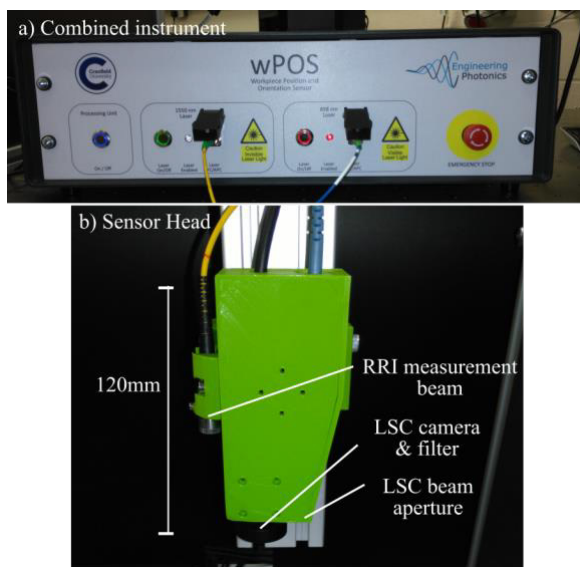


Fig. 3. a) Photograph of wPOS instrument and b) prototype sensor head.

reflecting surface with patterns possible from a wide variety of surfaces including metal, paper, sand and rocks [12].

### 2.3. Workpiece positioning sensor (wPOS)

The combination of both techniques allows a three degree-of-freedom positioning sensor, where the workpiece range information from the RRI sensor is also used to determine the optimal laser speckle calibration at any given point.

The combined instrument has been packaged into a 19" rack mount case containing power supplies, light sources (RRI: telecoms diode operating at 3mW, 1550nm, LSC: temperature stabilized laser diode operating at 0.5mW, 658nm) and signal processing hardware (FPGA, ADC and control PC) for both RRI and LSC, as shown in Fig. 3. The combined sensor head consists of USB3.0 camera and beam conditioning optics mounted in a 3D printed PLA plastic mount. Connection to the instrument is via a USB3 camera cable and armored optical fibre leads for light delivery.

## 3. Application areas and example results

### 3.1. Tool speed measurement.

In many continuous machining or processing operations the feed rate or tool speed is critical to process quality [2], and we have recently reported on the use of LSC to provide real-time tool speed measurements [8,13] for path characterization of a KUKA KR150 L110/2 industrial robot used for robotic wire and arc additive manufacturing (WAAM) [14]. In this work, oscillatory wall building paths were assessed prior to the build process to compensate for robotic motion errors, with unexpected reductions of tool speed of up to 25% observed. This is shown in Fig. 4 where the measured path is shown on the left-hand axis and the measured  $x$ ,  $y$  velocities and overall tool speed shown on the right. Here a reduction in travel speed is observed at corners, which unless compensated

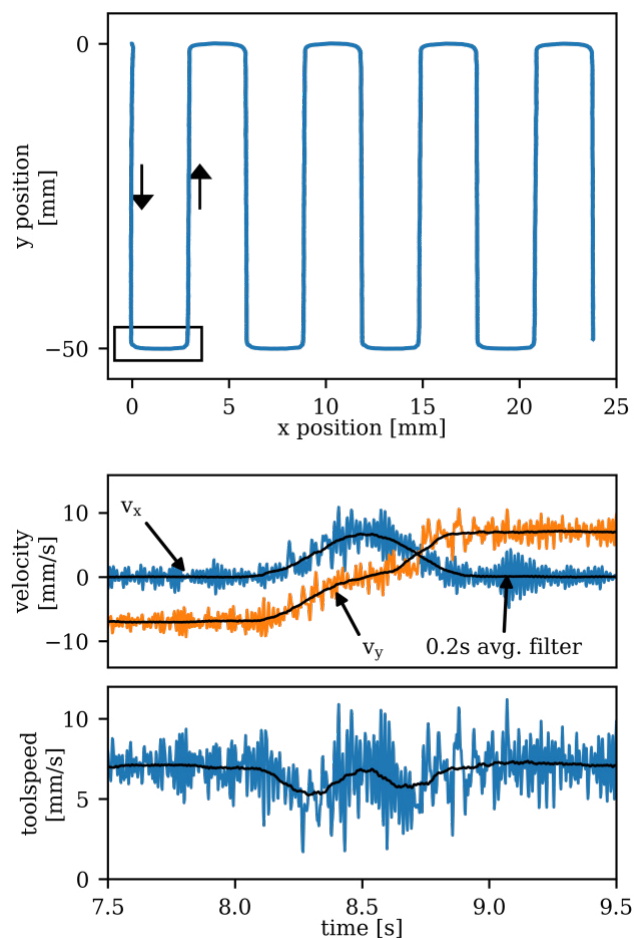


Fig. 4. Characterization of robotic paths for oscillatory wall building in the Wire and Arc additive manufacturing process.

for via wire-feed rate will result in an uneven surface profile in the built part [13]. The performance of the sensor used was investigated in [8] with the sensor accuracy found to have high accuracy with a maximum error of  $\pm 0.01$  mm/s over tool speeds of  $\pm 70$  mm/s.

### 3.2. In-process range measurement

Further potential areas of application are in-process range measurements for layer height measurement in additive manufacturing, cut depth and focus control in laser processing and workpiece shape measurement in robotic machining. An example of a trial application is shown in Fig. 5, which demonstrates the use of the RRI technique for layer height measurement in the WAAM process [14]. Here two consecutive layers were deposited with on-line measurements of the layer height made using the RRI absolute ranging mode during the build process. The layer height measurements are shown in Fig. 5 a) and a photograph of the resulting wall shown in Fig. 5 b). This measurement, made on-line in the presence of the welding arc, demonstrates the immunity of the RRI approach to high levels of background light.

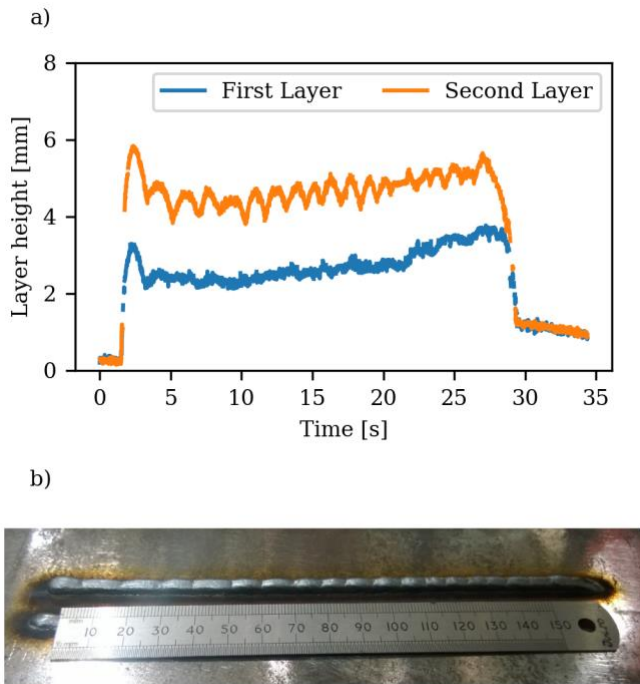


Fig. 5. a) In-process RRI measurement of layer height in Wire and Arc additive manufacturing. b) Photograph of the second layer of the test wall, where the correspondence to the second layer in a) can also be inspected.

### 3.3. Real-time positioning

In-plane positioning can be made via the LSC technique and in this mode the position is continuously tracked from a starting point with the reference speckle pattern updated when the translation is greater than the dimensions of the region of the camera chip used. Each re-referencing operation will therefore add to the measurement error and as such the error in the measurement will accumulate with distance. Therefore, the performance of the system can be categorized separately for short-range positioning or in-plane vibration measurement (length scales < cm) without re-referencing and for longer range positioning (length scales ~m) with re-referencing. Fig 6. shows an example of short range, high bandwidth measurement (10kHz) using LSC. Here an untreated aluminum sheet was translated by  $\pm 100\mu\text{m}$  using a translation stage and returned to the original position, as shown by the inset axis, measured to better than  $\pm 0.50\mu\text{m}$ .

This short range mode relies on continuously tracking relative to a fixed reference speckle pattern. Hence, the range will be limited by the size of this pattern with a maximum speckle shift of  $\frac{1}{2}$  the sensor size used. For a typical sensor head geometry, the speckle shift is approximately twice the translation [7] giving a maximum translation of  $\sim \frac{1}{4}$  of the image dimensions. For example, for an image size of  $512 \times 512$  pixels with a typical pixel size of  $4.8\mu\text{m}$  the image size is  $\sim 2.4\text{mm}$  and the maximum speckle shift is  $1.2\text{mm}$  and the translation will be limited to approximately  $\pm 0.6\text{mm}$ . The bandwidth will depend upon the camera data rate and

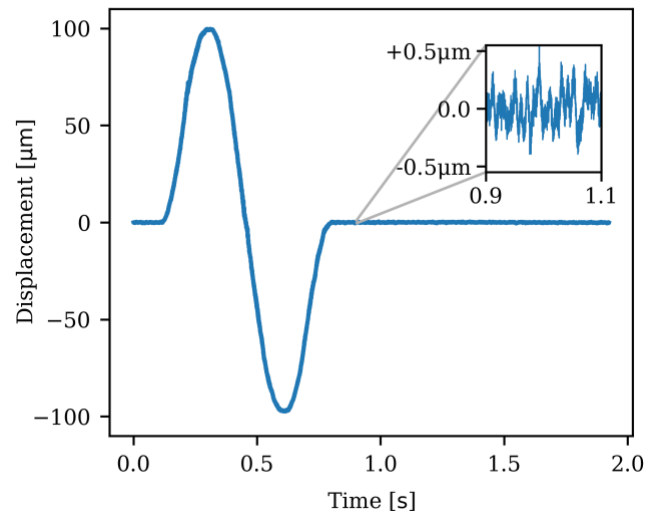


Fig. 6. An example of short-range, high bandwidth, in-plane displacement measurement using LSC.

achievable correlation rate with smaller images allowing higher data rate but lower maximum translations.

As mentioned above longer range positioning requires re-referencing operations with the resulting accumulation of position error with distance. An example of measured robot path using this approach is shown in Fig. 7 for the WAAM oscillatory wall path described in section 3.1 above with the robot returning diagonally to the starting position at (0,0) mm. Here multiple measurements of the same robot program are shown overlaid demonstrating a repeatability of  $< 10\mu\text{m}$ . The zoomed axes on the right of Fig. 7 show various regions on the path; the top-right shows the robots starting and ending position as measured by the sensor while the middle plot shows measurement of the robot vibration and the lower plot shows a close up of the robot path at corners.

The offset between starting and ending positions of  $\sim 120\mu\text{m}$  after  $\sim 0.5\text{m}$  travel is believed to be due to the measurement error introduced by a slight change in working height due to misalignment between the build plate and robot  $xy$  plane. Such a variation can lead to miscalibration errors in the LSC process due to slight changes in the scaling factors used to convert measured speckle shift to translation.

To correct for this effect, the range information provided by the RRI ranging mode can be used to automatically correct the scaling factors used, an approach that is currently under investigation. In this approach the sensor is calibrated at a number of different working heights, covering the expected range of operation, typically between  $\pm 5\text{mm}$  from the designed working distance. At each working height the scaling factors are measured by the application of repeated controlled displacements in both  $x$  and  $y$  directions independently using a high-accuracy translation stage. During measurements the speckle shift is first found using normalized cross-correlation, along with the  $z$  position measurement from the RRI system. The scaling factors for the conversion of the speckle shift to sensor translation are then found from the calibrated values together with linear interpolation between the calibrated  $z$  positions.



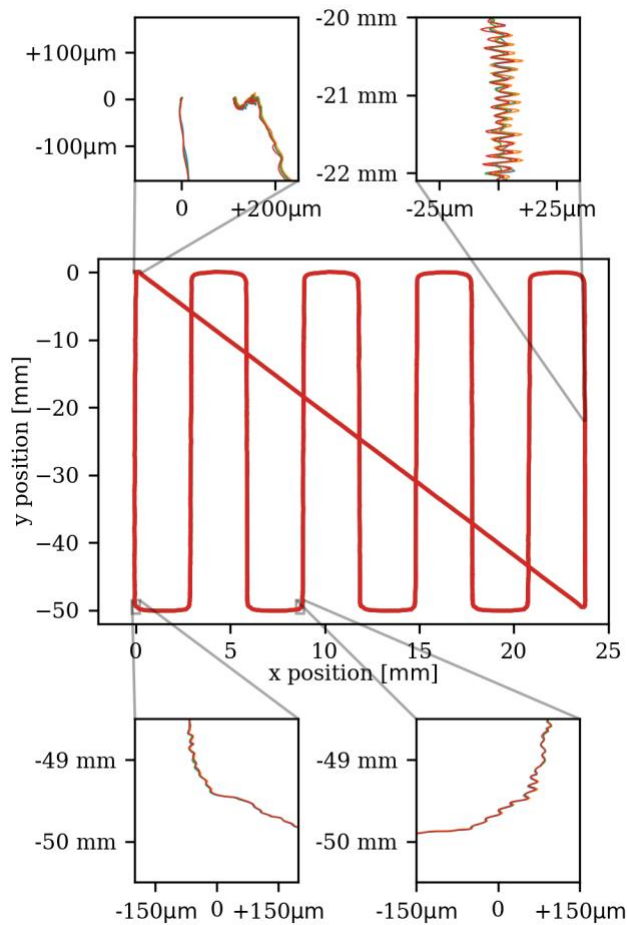


Fig. 7. Measured robot path used for WAAM oscillatory wall building. Here multiple measurements are overlaid showing repeatability of the robot path and sensor.

The results of a trial in the laboratory using a fixed sensor and moving aluminum plate mounted on a 6 degree-of-freedom translation stage system are shown in Fig. 8. Here a rectangular path 175 x 200 mm (total travel = 0.75m) was traversed with an artificial 1mm height change between two sides of the rectangle. Fig. 8 a) shows the measured position and Fig 8 b) shows magnified axes centered on the start/end position. Multiple measurements are overlaid to demonstrate the sensor repeatability of  $\sim 15 \mu\text{m}$ , and the accuracy can be assessed by the offset from (0,0) mm position to be  $< 15 \mu\text{m}$  after 0.75m travel. The design of the sensor head can be further optimized to ensure that the range measurement used to find the speckle scaling factors is made at the same surface position as the laser speckle measurement. If there is any difference in the surface range between the two measurements points this will introduce errors in the scaling factors used in the calculation of the in-plane position resulting in increased positioning errors. This can be seen in Fig. 9 where the height change is now applied as a constant gradient change between

the two sides. Here the performance is worse due to the offset between the RRI and LSC measurement points of  $\sim 10\text{mm}$ . Here the accuracy, assessed by the offset from the origin, is now  $< 30 \mu\text{m}$  after 0.75m travel.

#### 4. Conclusions

In this paper we have presented the two measurement techniques, Range Resolved Interferometry and Laser Speckle Correlation and their combination in an instrument capable of measurement of the three translation degrees-of-freedom for robotic positioning feedback and process-monitoring. Different potential application areas for the combined instrument or the individual measurement techniques have been proposed and examples of preliminary trials in these areas presented. These application area/measurement modes are summarized in Table 1.

Future development of the instrument will investigate the optimization of in-plane positioning performance improvements and out-of-plane range resolution via the RRI approach and optimization of the LSC technique for in-process measurements in the presence of strong process light.

Table 1. Summary of measurement modes and performance.

Measurement mode	Notes/ Typical performance
In-plane tool speed	2D velocity measurement via LSC. $\pm 0.01 \text{ mm/s}$ accuracy over tool speeds of $\pm 70 \text{ mm/s}$ ,
Out-of-plane positioning/range	RRI ranging mode. $\sim 10$ to $100 \mu\text{m}$ resolution (100mm working range) at kHz data rates.
Out-of-plane displacement/vibration [15]	RRI interferometric processing mode. $\sim 1$ -10 nm resolution, typical at 20kHz bandwidth
In-plane positioning/displacement/vibration (short range $\sim \text{mm}$ to $\text{cm}$ )	LSC (+ working distance correction via RRI ranging mode.) $< 0.5 \mu\text{m}$ , up to $\sim 10\text{kHz}$
In-plane positioning (long range $\sim 1\text{m}$ )	LSC (+ working distance correction via RRI ranging mode.) $\sim 120 \mu\text{m/m}$

#### Acknowledgements

This work was supported by the Engineering and Physical Sciences Research Council (EPSRC) UK [grant numbers EP/M020401/1, EP/ N002520/1].

The authors would like to acknowledge our colleagues in the Welding Engineering and Laser Processing Centre, Cranfield University for collaborations involving the WAAM process.

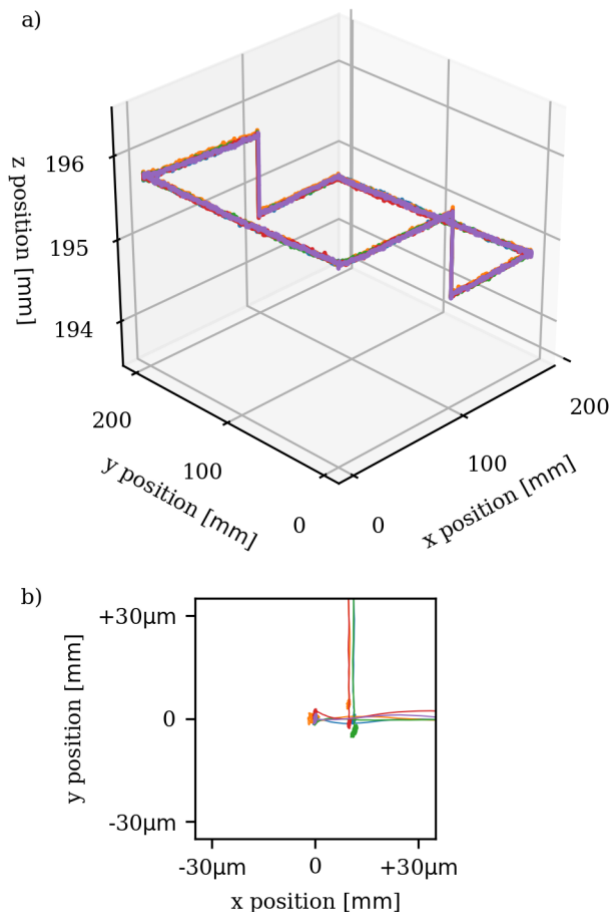


Fig. 8. a) 3d position measurements for a rectangular path with a 1 mm height change applied as a step change between the two-sides. Here multiple measurements are overlaid showing repeatability of the robot path and sensor. b) Shows the offset error in final measured position after returning to the origin.

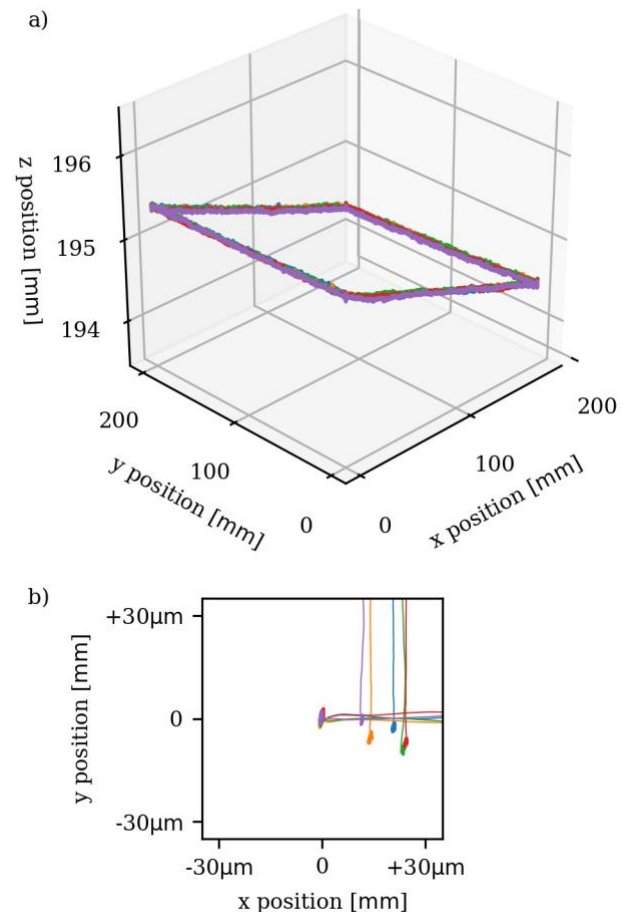


Fig. 9. a) 3d position measurements for a rectangular path with a 1 mm height change applied as a gradient change between the two-sides. Here multiple measurements are overlaid showing repeatability of the robot path and sensor. b) Shows the offset error in final measured position after returning to the origin.

## References

- [1] Brogardh T. Present and future robot control development: An industrial perspective, *Annual Reviews in Control*, 2007; 31: pp: 69–79.
- [2] Chen Y, Dong F. Robot machining: Recent development and future research issues, *International Journal of Advanced Manufacturing Technology*, 2013; 66: pp: 1489–1497.
- [3] Bauer J, Friedmann M, Hemker T. Analysis of Industrial Robot Structure and Milling Process Interaction for Path Manipulation in Process Machine Interactions, Berlin-Heidelberg, Springer; 2013.
- [4] Kanko JA, Sibley AP, Fraser JM. In situ morphology-based defect detection of selective laser melting through inline coherent imaging,” *J. Mater. Process. Technol.*, 2016; 231: pp: 488–500.
- [5] Zaeh M, Hatwig J, Musiol J. Analysis of the Accuracy of Industrial Robots and Laser Scanners for Remote Laser Beam Welding and Cutting, 41st Int. Symp. and 6th Ger. Conf. Robot., Munich, Germany, VDE; 2010: pp: 751–758.
- [6] Kissinger T, Charrett TOH, Tatam RP. Range-resolved interferometric signal processing using sinusoidal optical frequency modulation, *Opt. Express*, 2015; 23(7): pp: 9415–9431.
- [7] Yamaguchi I. Speckle Displacement and Decorrelation in the Diffraction and Image Fields for Small Object Deformation, *Opt. Acta Int. J. Opt.*, 1981; 28(10): pp: 1359–1376.
- [8] Charrett TOH, Bandari YK, Michel F, Ding J, Williams SW, Tatam RP. A non-contact laser speckle sensor for the measurement of robotic tool speed, *Robot. Comput. Integr. Manuf.*, 2018; 53: pp: 187–196.
- [9] Charrett TOH, Kotowski K, Tatam RP. Speckle tracking approaches in speckle sensing, *SPIE Opt. + Optoelectron.*, Prague, Czech Rep., in *SPIE Proceedings Vol. 1023*, 2017; pp: 102310L.
- [10] Berkovic G, Shafir E. Optical methods for distance and displacement measurements, *Adv. Opt. Photonics*, 2012; 4(4): pp: 441–471.
- [11] Lewis JP. Fast normalized cross-correlation, *Vis. Interface*, 1995; 10(1): pp: 120–123.
- [12] Charrett TOH, Waugh L, Tatam RP. Speckle velocimetry for high accuracy odometry for a Mars exploration rover, *Meas. Sci. Technol.*, 2010; 21(2): 025301.
- [13] Bandari YK, Charrett TOH, Michel F, Ding J, Williams SW, Tatam RP. Compensation strategies for robotic motion errors for additive manufacturing (AM), *Int. Solid Free. Fabr. Symp.*, Austin, Texas, 2016.
- [14] Williams SW, Martina F, Addison AC, Ding J, Pardal G, Colegrove P. Wire + Arc Additive Manufacturing, *Mater. Sci. Technol.* 2016; 32(7): pp: 641–647.
- [15] Kissinger T, Charrett TOH, James SW, Adams A, Twin A, Tatam RP. Simultaneous laser vibrometry on multiple surfaces with a single beam system using range-resolved interferometry, *Proc. SPIE 9525, Opt. Meas. Syst. Ind. Insp. IX*, 2015; pp: 952520.

2019-03-13

# Workpiece positioning sensor (wPOS): A three-degree-of-freedom relative end-effector positioning sensor for robotic manufacturing

Charrett, Thomas O. H.

Elsevier

---

Charrett T, Kissinger T, Tatam R. (2019) Workpiece positioning sensor (wPOS): A three-degree-of-freedom relative end-effector positioning sensor for robotic manufacturing. Procedia CIRP, Volume 79, pp. 620-625

<https://doi.org/10.1016/j.procir.2019.02.078>

*Downloaded from Cranfield Library Services E-Repository*